Supporting information

Self-assemblies of Zinc-complexes for Aggregation Induced Emission Luminogen Precursors

Rinki Brahma, Jubaraj B. Baruah*

Department of Chemistry, Indian Institute of Technology Guwahati, Guwahati -781 039, Assam, India. Email: juba@iitg.ac.in

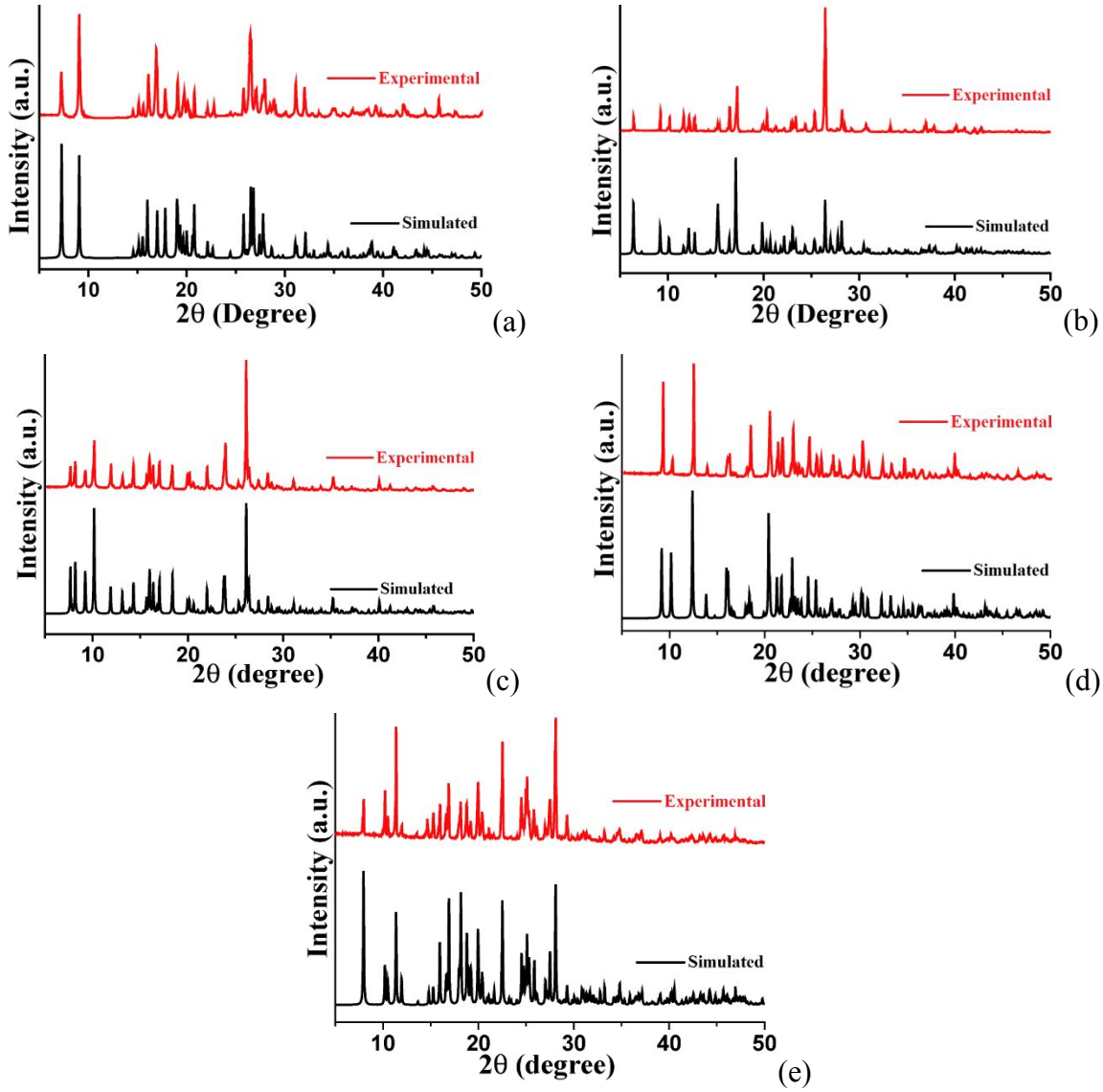

Figure S1: PXRD patterns of (a) Complex **1**; (b) Complex **2**; (c) Complex **3**; (d) Complex **4** (e) Complex **5** and simulated patterns generated from CIF file (Red = Experimental, Black = Simulated).

Quantum yield calculation of aggregation induced emission in solution:

The quantum yield of fluorescence was determined by using quinine sulphate as a reference in DMSO at room temperature.

$$Quantum\ Yield = \frac{Area\ of\ the\ complex}{Area\ of\ Quinine\ Sulphate} x \frac{Absorbance\ \ at\ 333nm\ (Quinine\ Sulphate)}{Absorbance\ \ at\ 333nm\ (Complex)} x \frac{\eta^2}{\eta_R^2} x\ Q_R$$

where, η = Refractive Index of solvent used of sample preparation
η_R = Refractive Index of solvent used of reference preparation

Q_R = Quantum yield of reference

Crystallographic Study: X-ray single crystal diffraction data of the complexes **1** and **2** were collected on an Oxford SuperNova diffractometer whereas for the complexes **3**, **4** and **5** were collected by using a Bruker Nonius SMART APEX CCD diffractometer equipped with a graphite monochromator. The data were collected at 296 K with Mo Kα radiation (λ = 0.71073 A). Data reduction and cell refinement were carried out by CrysAlisPro software. Structures were solved using SHELXS-14 by direct method and refined by full-matrix least-squares on F^2 using SHELXL-14. All non-hydrogen atoms were refined in anisotropic approximation against F^2 of all reflections. Hydrogen atoms were placed at their geometric positions by riding and refined in the isotropic approximation. The crystallographic parameters are listed in table 1S. (Reference : Sheldrick GM. ActaCrystallogr. C Struct. Chem. **2015**, *71*, 3 - 8.)

Table S1: Crystallographic parameters of the complexes **1-5**

Parameters	Complex **1**	Complex **2**	Complex **3**	Complex **4**	Complex **5**
Formula	$C_{28}H_{28}N_6O_{12}Zn$	$C_{26}H_{22}N_6O_{11}Zn$	$C_{42}H_{36}N_8O_{20}Zn_2$	$C_{26}H_{28}N_6O_{14}Zn$	$C_{20}H_{20}N_4O_{12}Zn$
CCDC	1964042	1964041	1964043	1964039	1964040
Mol.wt.	705.93	659.86	1103.53	713.91	573.77
Space group	C 2/c	P -1	C 2/c	P 2_1/n	P -1
a(Å)	20.1428(11)	8.0671(6)	22.0343(8)	7.8574(4)	5.9866(7)
b(Å)	6.2816(3)	12.718(2)	13.6328(5)	19.2849(9)	8.7293(10)
c (Å)	25.1031(13)	14.3069(18)	15.1548(6)	9.9755(5)	22.354(3)
α (°)	90	81.172(13)	90	90	96.624(3)
β (°)	104.399(5)	76.060(9)	100.7150(10)	102.3550(10)	90.797(4)
γ (°)	90	74.624(12)	90	90	90.264(3)
V (Å^3)	3076.5(3)	1367.3(3)	4473.0(3)	1476.57(13)	1160.2(2)
Density, g cm^{-3}	1.524	1.603	1.639	1.606	1.642
Abs. coeff., mm^{-1}	0.872	0.972	1.165	0.914	1.133
F (000)	1456	676	2256	736	588
Total no. of reflections	2736	4830	3966	2617	4117
Reflections, I > 2σ(I)	2221	3589	3065	2299	3653
Max. θ/°	25.049	25.044	25.044	25.047	25.050
Ranges (h, k, l)	$-23 \le h \le 15$	$-9 \le h \le 9$	$-26 \le h \le 26$	$-9 \le h \le 9$	$-7 \le h \le 7$
	$-6 \le k \le 7$	$-10 \le k \le 15$	$-16 \le k \le 16$	$-22 \le k \le 22$	$-10 \le k \le 10$
	$-23 \le l \le 29$	$-17 \le l \le 15$	$-18 \le l \le 18$	$-11 \le l \le 11$	$-26 \le l \le 26$
Complete to 2θ (%)	99.9	99.9	100	100	100
Data/restraints/parameters	2736/0/223	4830/2/413	3966/2/338	2617/4/227	4117/2/357
GooF (F^2)	1.038	1.007	1.040	1.025	1.012
R indices [I > 2σ(I)]	0.0406	0.0523	0.0318	0.0256	0.0544
wR_2 [I > 2σ(I)]	0.0788	0.0992	0.0877	0.0503	0.1793
R indices (all data)	0.0552	0.0755	0.0469	0.0311	0.0623
wR_2 (all data)	0.0861	0.1178	0.0979	0.0528	0.1902

Table S2: Solid state fluorescence emissions λ_{ex} (350 nm) and quantum yield of metal complexes **1-5**.

Complexes	λ_{em} (nm)	Quantum yield (%)
Complex **1**	434, 463	1.48
Complex **2**	437	4.14
Complex **3**	438, 463	2.61
Complex **4**	439	13.56
Complex **5**	448	0.56

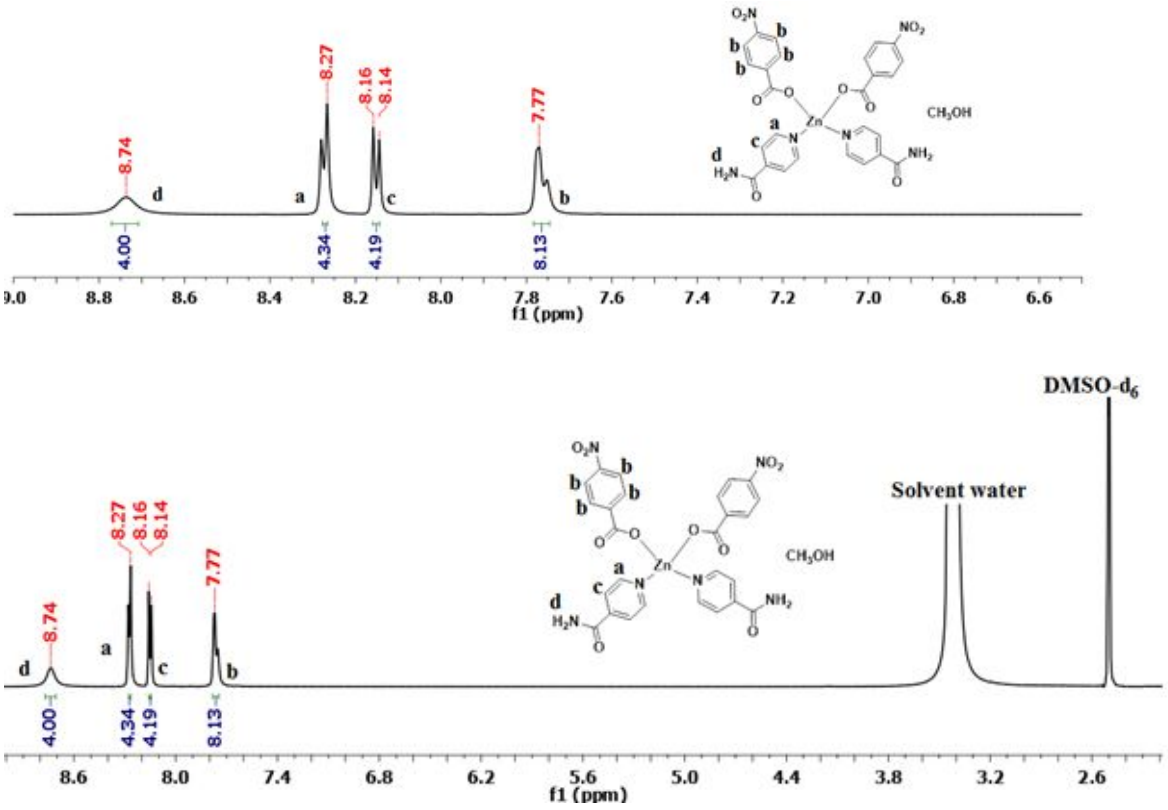

Figure S2: ^{1}H-NMR (600 MHz, DMSO-d_6) spectra of complex **1** (top: expansion of aromatic region).

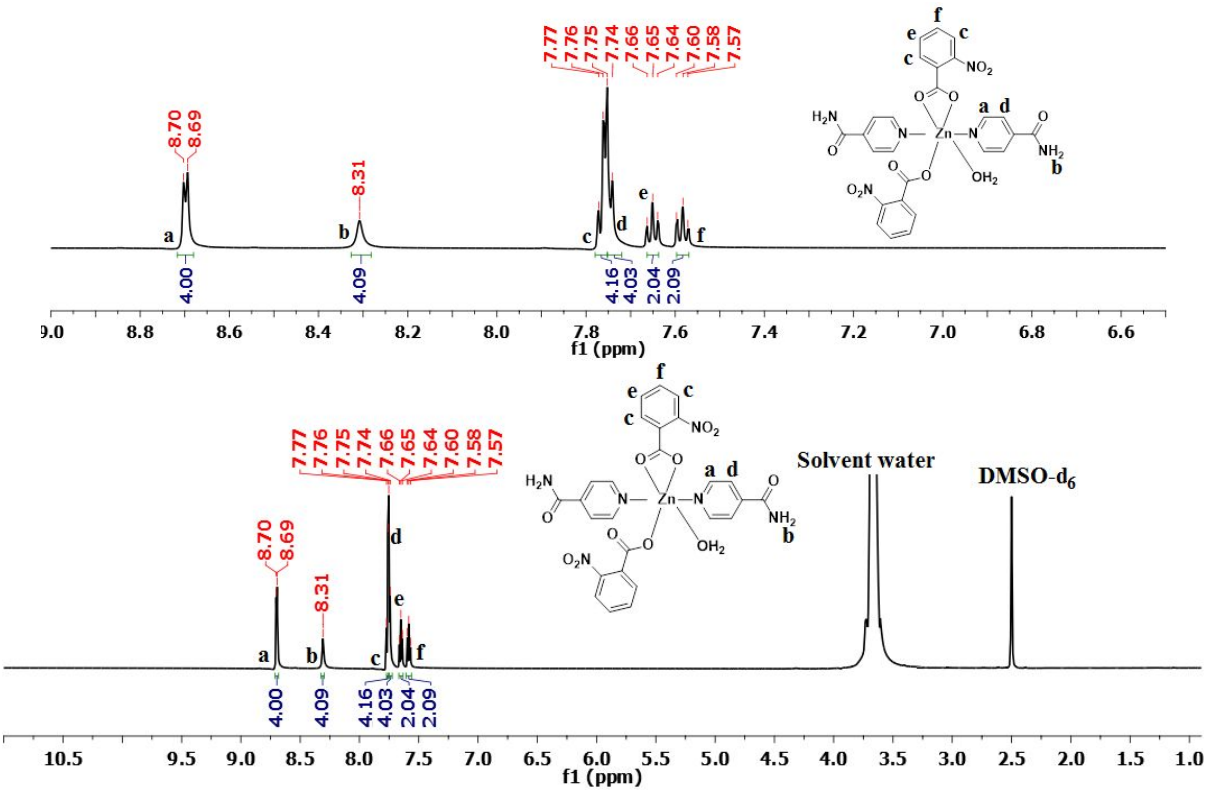

Figure S3: ^{1}H-NMR (600 MHz, DMSO-d_6) spectra of complex **2** (top: expansion of aromatic region).

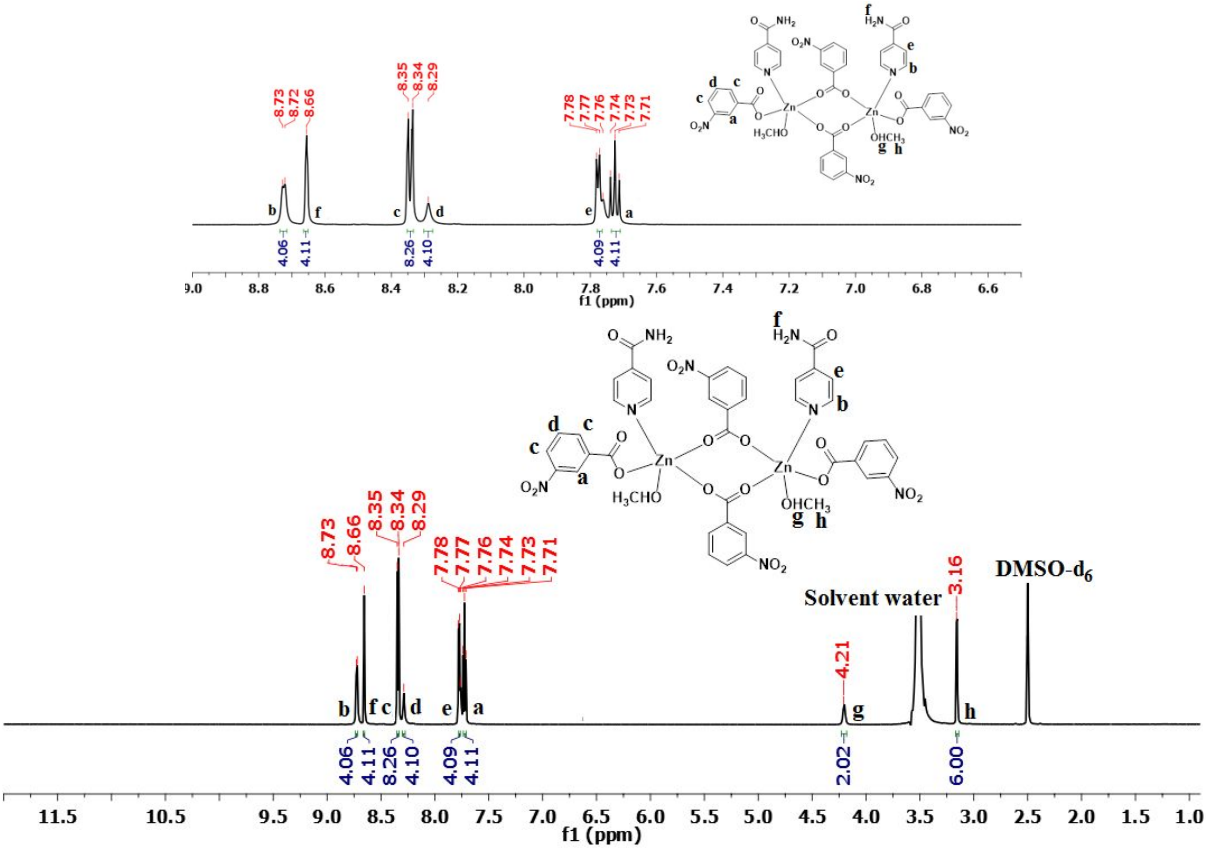

Figure S4: ^{1}H-NMR (600 MHz, DMSO-d_6) spectra of complex **3**. (top: expansion of aromatic region).

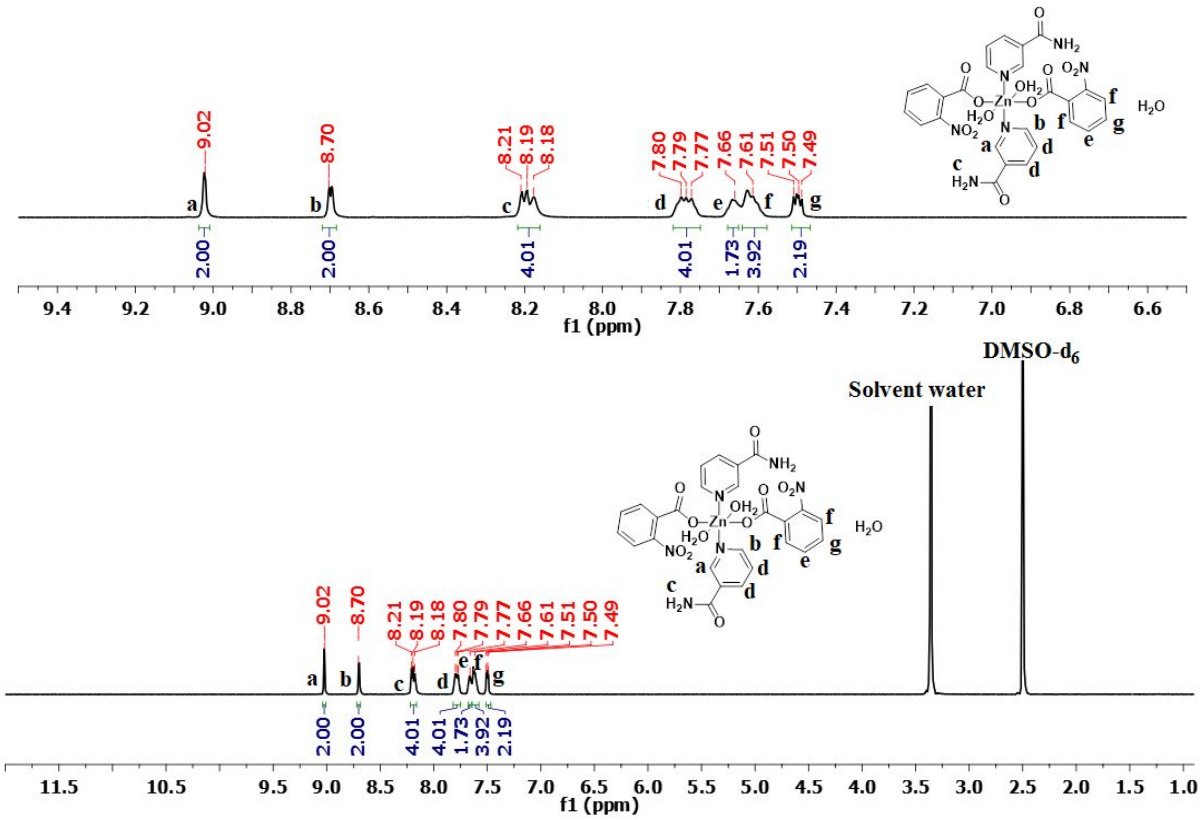

Figure S5: ^{1}H-NMR (600 MHz, DMSO-d_6) spectra of complex **4**. (top: expansion of aromatic region).

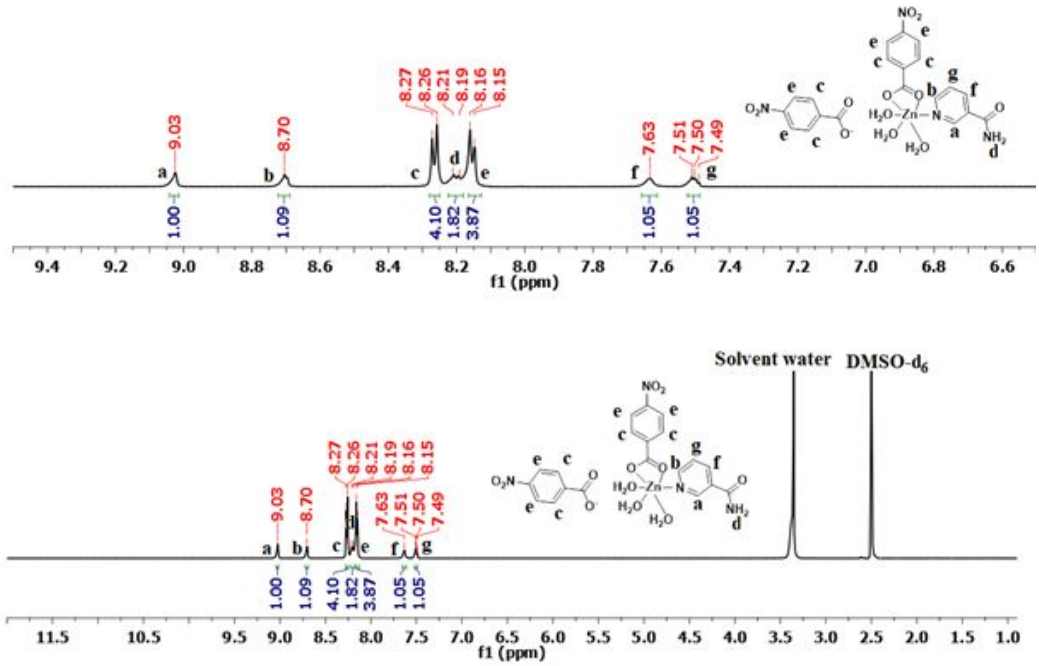

Figure S6: ^{1}H-NMR (600 MHz, DMSO-d_6) spectra of complex **5** (top: expansion of aromatic region).

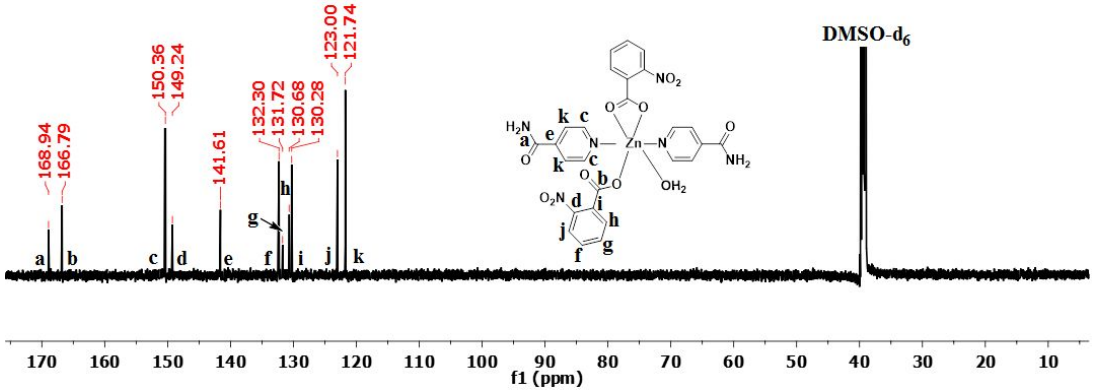

Figure S7: ^{13}C-NMR (100 MHz, DMSO-d$_6$) spectra of complex **2**.

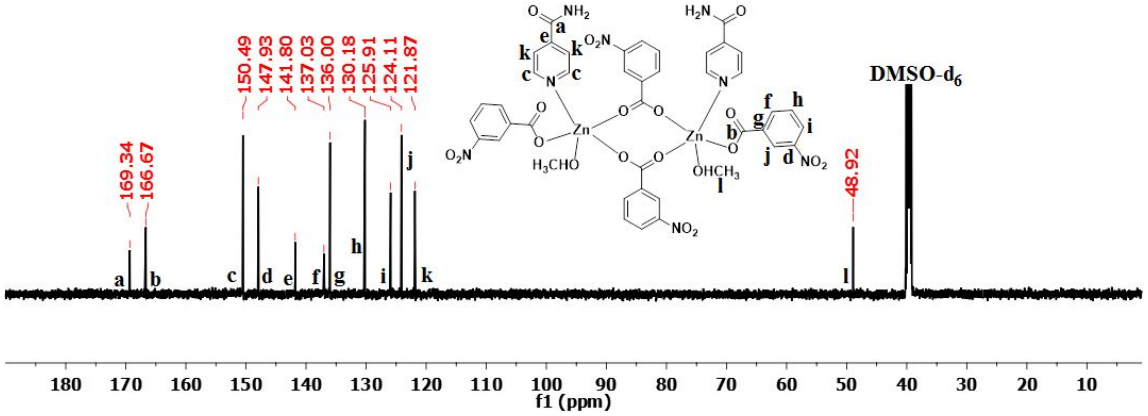

Figure S8: ^{13}C -NMR (100 MHz, DMSO-d$_6$) spectra of complex **3**.

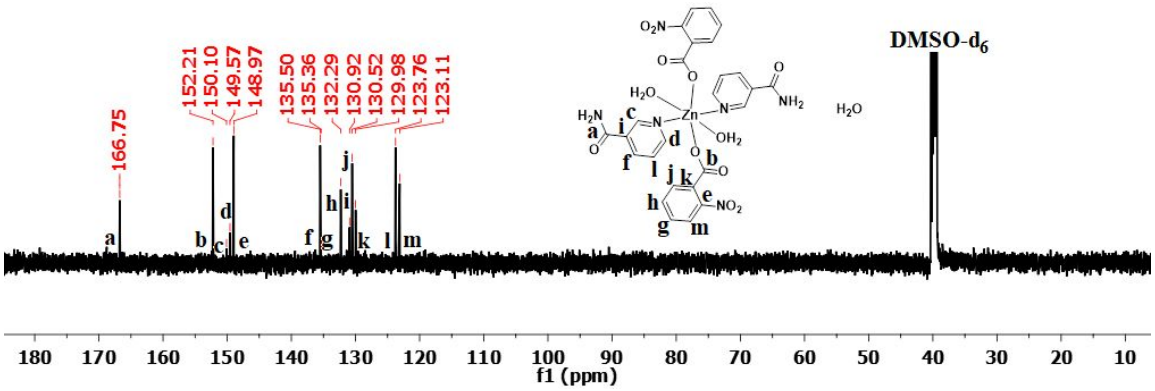

Figure S9: ^{13}C -NMR (100 MHz, DMSO-d$_6$) spectra of complex **4**.

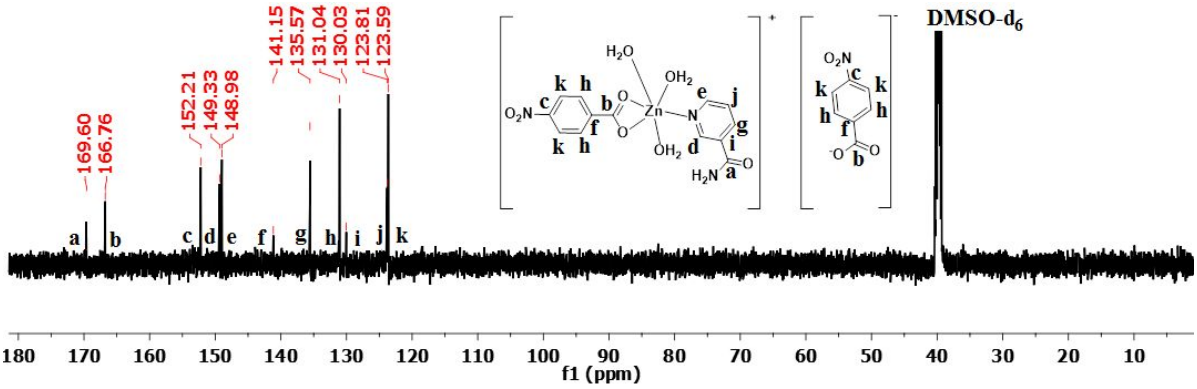

Figure S10: ^{13}C -NMR (100 MHz, DMSO-d_6) spectra of complex **5**.

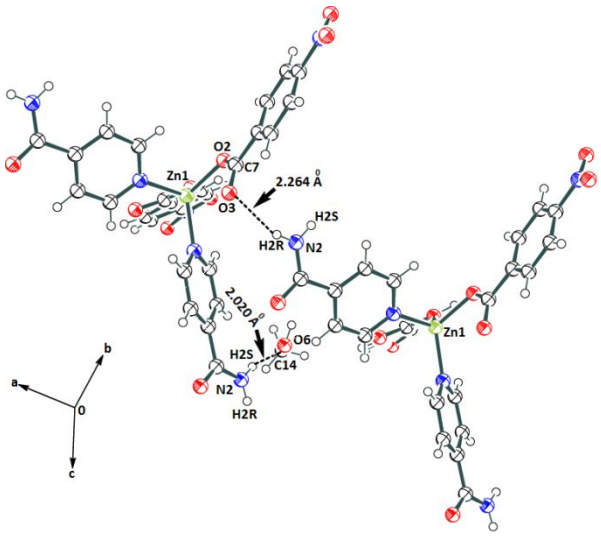

Figure S11: Hydrogen-bonded self-assembly of complex **1**.

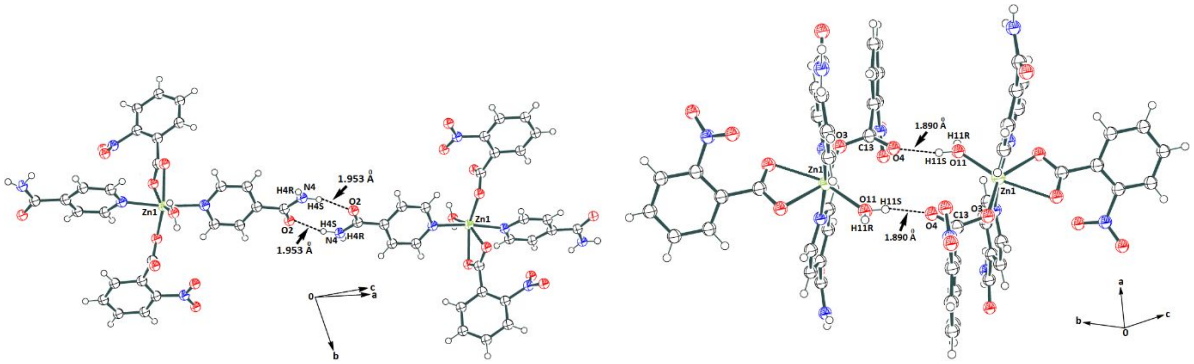

Figure S12: Hydrogen-bonded self-assembly of complex **2**.

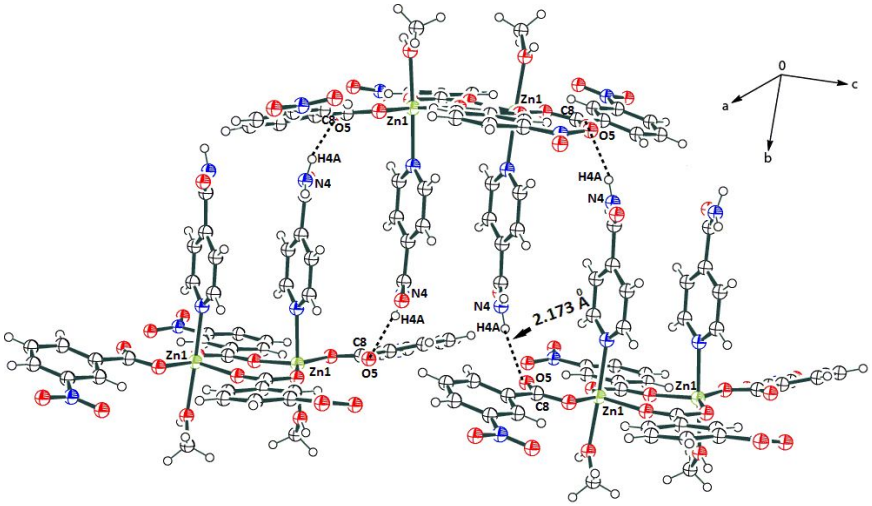

Figure S13: Hydrogen-bonded self-assembly of complex **3**.

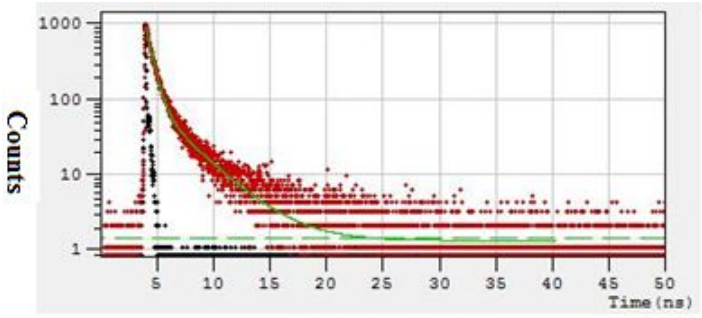

Goodness of fit χ^2: 1.002

	B_i	ΔB_i	f_i (%)	Δf_i (%)	τ_i (ns)	$\Delta \tau_i$ (ns)
1	829.5481	4.5726	62.131	1.951	0.558	0.014
2	93.3513	2.2231	37.869	0.963	3.025	0.005

Figure S14: Time resolved fluorescence emission of solid sample of the complex **1** (λ_{ex}= 375 nm, λ_{em}= 434 nm).

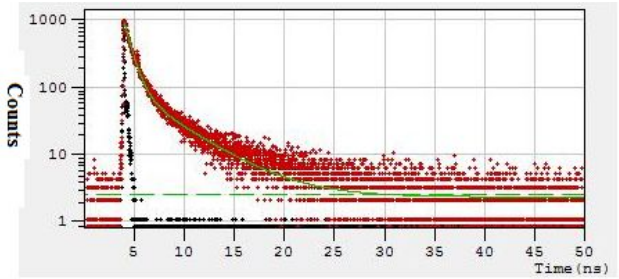

Goodness of fit χ^2: 1.314

	B_i	ΔB_i	f_i (%)	Δf_i (%)	τ_i (ns)	$\Delta \tau_i$ (ns)
1	834.0839	4.7036	59.178	1.239	0.727	0.011
2	97.2193	2.0364	40.822	0.885	4.302	0.003

Figure S15: Time resolved fluorescence emission of solid sample of complex **1** (λ_{ex}= 375 nm, λ_{em} = 463 nm).

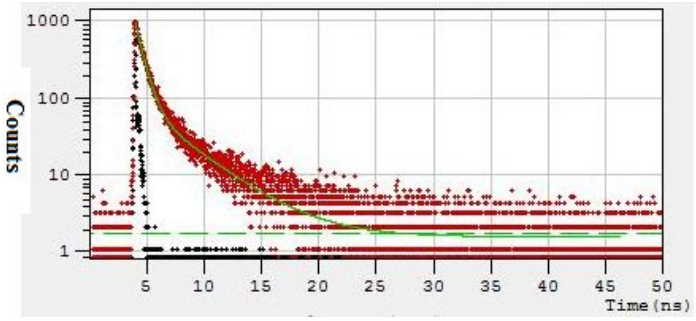

Goodness of fit χ^2: 1.038

	B_i	ΔB_i	f_i (%)	Δf_i (%)	τ_i (ns)	$\Delta \tau_i$ (ns)
1	902.3928	4.3080	64.761	1.338	0.647	0.010
2	83.8453	1.7873	35.239	0.785	3.788	0.004

Figure S16: Time resolved fluorescence emission of solid sample of complex **2** (λ_{ex} = 375 nm, λ_{em} = 437 nm).

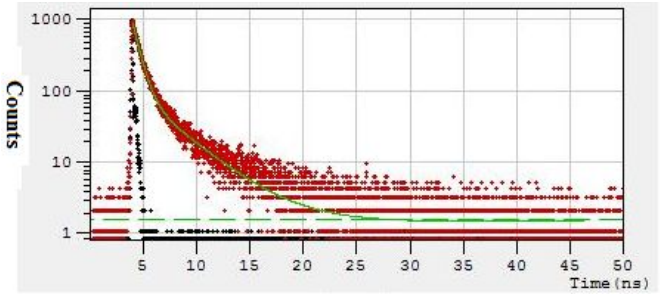

Goodness of fit χ^2: 1.041

	B_i	ΔB_i	f_i (%)	Δf_i (%)	τ_i (ns)	$\Delta \tau_i$ (ns)
1	847.6031	4.2602	61.732	1.405	0.641	0.011
2	94.7730	2.0011	38.268	0.848	3.554	0.004

Figure S17: Time resolved fluorescence emission of solid sample of complex **3** (λ_{ex}= 375 nm, λ_{em}= 438 nm).

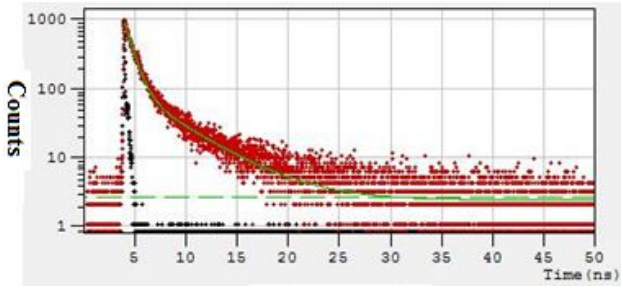

Goodness of fit χ^2: 1.364

	B_i	ΔB_i	f_i (%)	Δf_i (%)	τ_i (ns)	$\Delta \tau_i$ (ns)
1	803.3154	4.5451	58.256	1.126	0.775	0.011
2	98.0222	2.0397	41.744	0.896	4.553	0.003

Figure S18: Time resolved fluorescence emission of solid sample of complex **3** (λ_{ex}= 375 nm, λ_{em}= 463 nm).

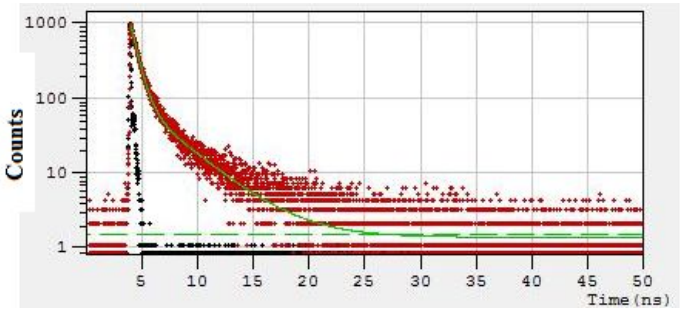

Goodness of fit χ^2: 1.025

	B_i	ΔB_i	f_i (%)	Δf_i (%)	τ_i (ns)	$\Delta \tau_i$ (ns)
1	861.7091	4.3212	61.555	1.493	0.607	0.012
2	93.2296	1.8667	38.445	0.809	3.506	0.004

Figure S19: Time resolved fluorescence emission of solid sample of complex **4** (λ_{ex} = 375 nm, λ_{em}= 439 nm).

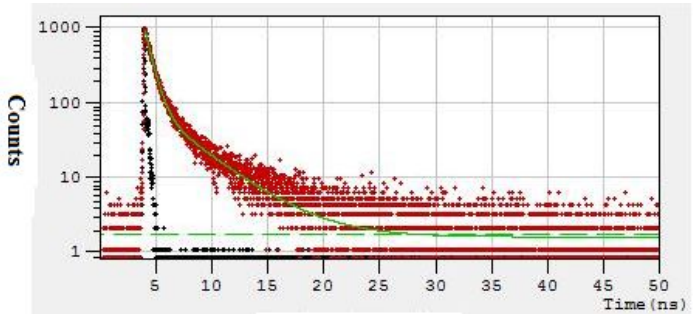

Goodness of fit χ^2 : 1.093

	B_i	ΔB_i	f_i (%)	Δf_i (%)	τ_i (ns)	$\Delta \tau_i$ (ns)
1	826.3301	4.1895	60.990	1.398	0.631	0.011
2	88.2730	1.7334	39.010	0.801	3.780	0.003

Figure S20: Time resolved fluorescence emission of solid-sample of complex **5** (λ_{ex} = 375 nm, λ_{em}= 448 nm).

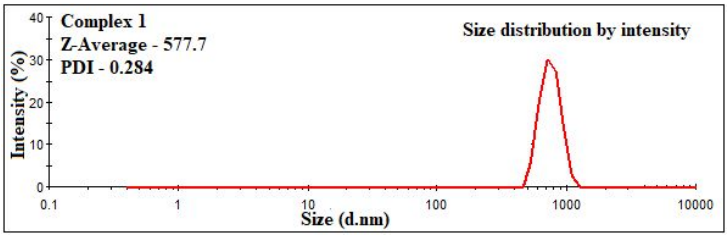

(a)

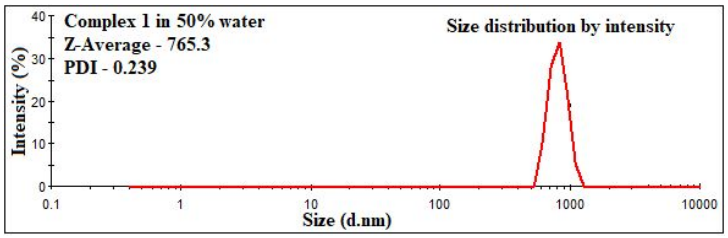

(b)

Figure S21: Plot of intensity vs size from dynamic light-scattering of complex **1** (10^{-4}M) (a) in DMSO and (b) in DMSO with 50% water.

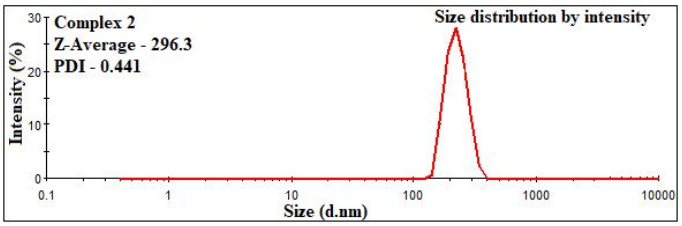

(a)

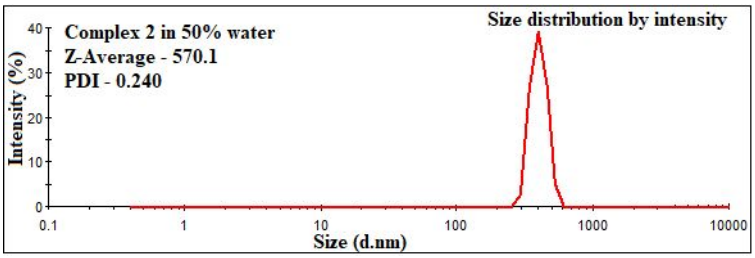

(b)

Figure S22: Plot of intensity vs size from dynamic light-scattering of the complex **2** (10^{-4}M) (a) in DMSO and (b) in DMSO with 50% water.

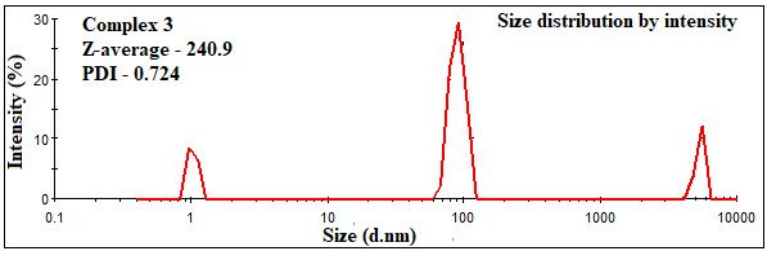

(a)

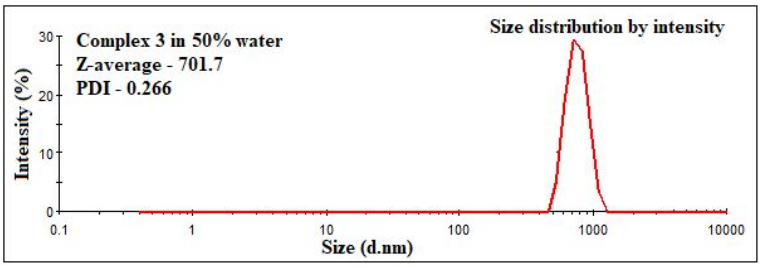

(b)

Figure S23: Plot of intensity vs size from dynamic light-scattering of complex **3** (10^{-4}M) (a) in DMSO and (b) in DMSO with 50% water.

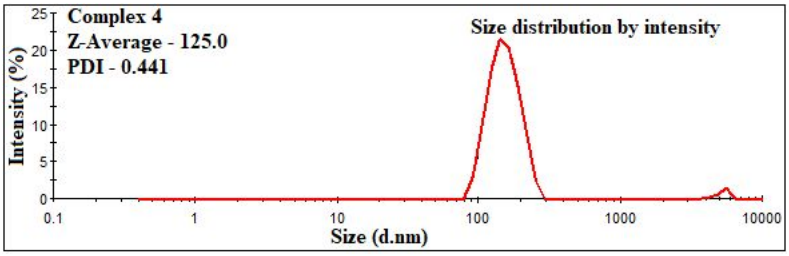

(a)

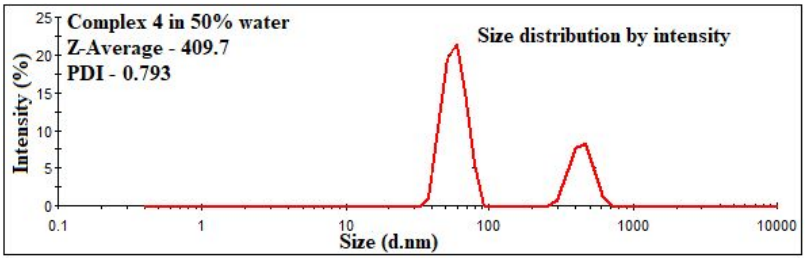

(b)

Figure S24: Plots of intensity vs size from dynamic light-scattering of complex **4** (10^{-4}M) (a) in DMSO and (b) in DMSO with 50% water.

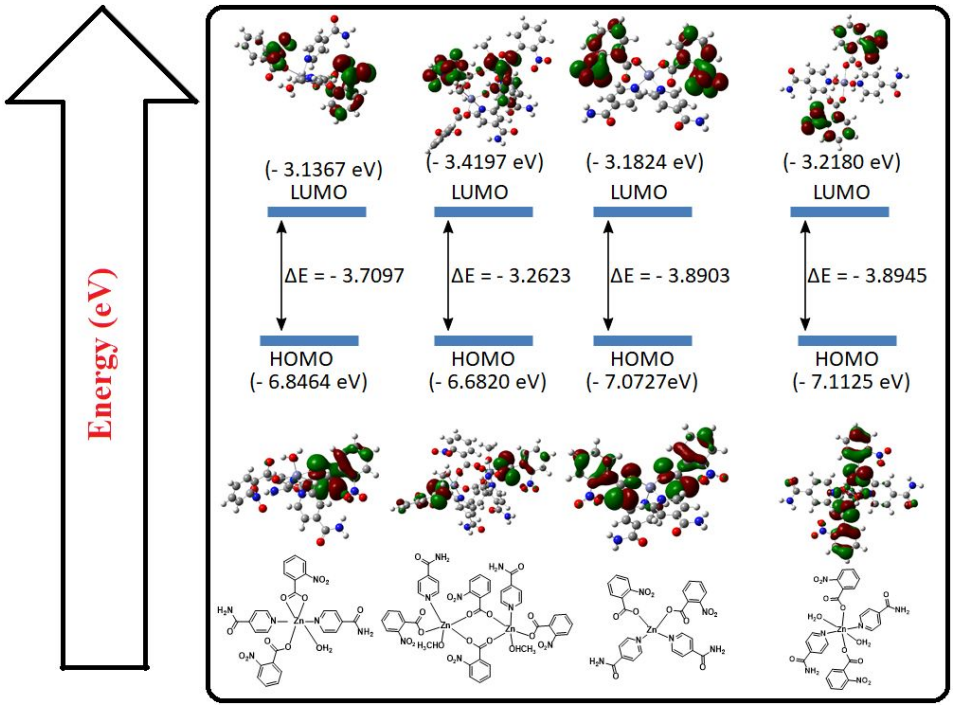

Figure S25: The HOMO and LUMO of zinc complexes having pyridine-4-carboxamide and 2-nitrobenzoate having different coordination, calculated by DFT using B3LYP function with LANL2DZ as basis set.

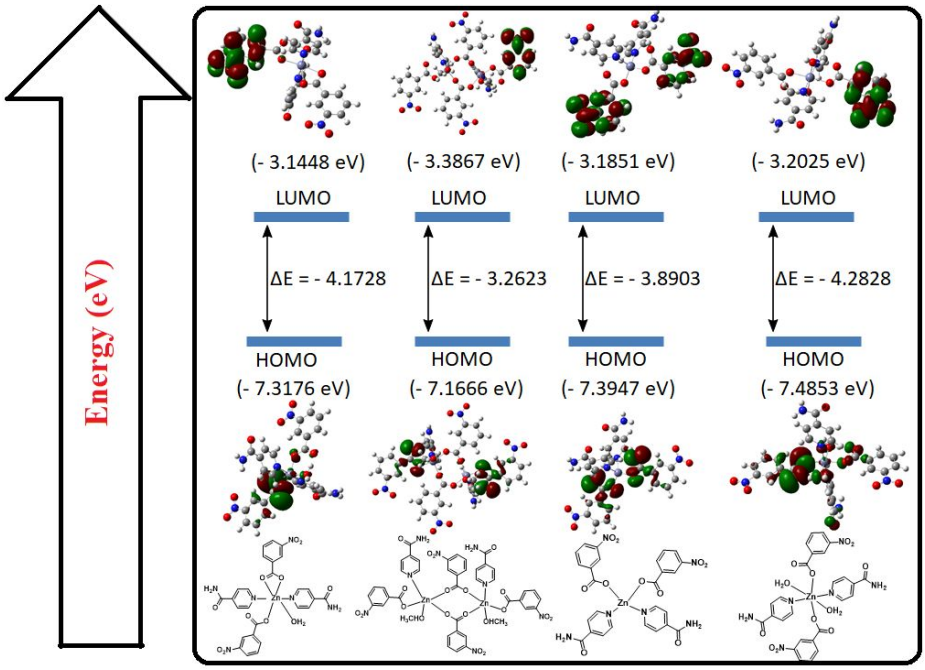

Figure S26: The HOMO and LUMO of different non-ionic zinc-complexes having pyridine-4-carboxamide and 3-nitrobenzoate, calculated by DFT using B3LYP function with LANL2DZ as basis set.

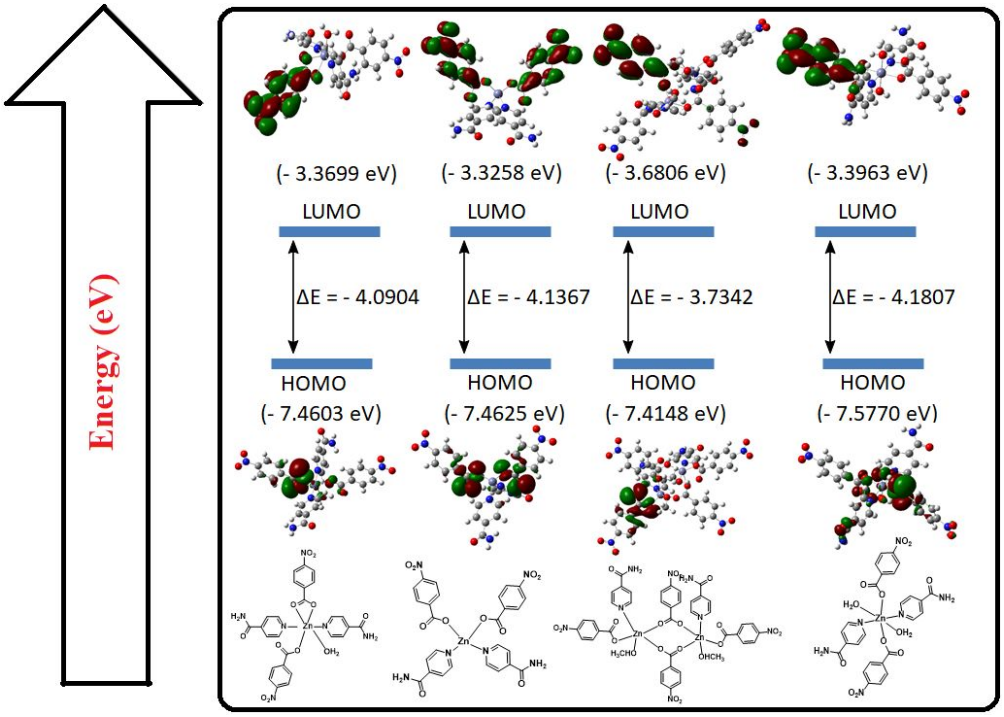

Figure S27: The HOMO and LUMO of different non-ionic zinc-complexes having pyridine-4-carboxamide and 4-nitrobenzoate complexes, calculated by DFT using B3LYP function with LANL2DZ as basis set.

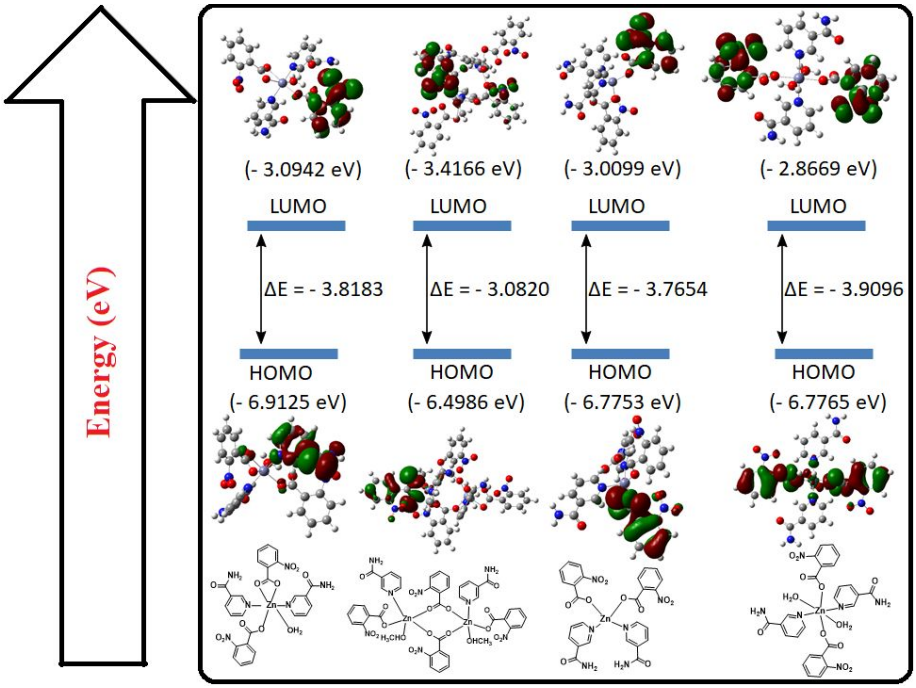

Figure S28: The HOMO and LUMO different non-ionic zinc-complexes having pyridine-3-carboxamide and 2-nitrobenzoate, calculated by DFT using B3LYP function with LANL2DZ as basis set.

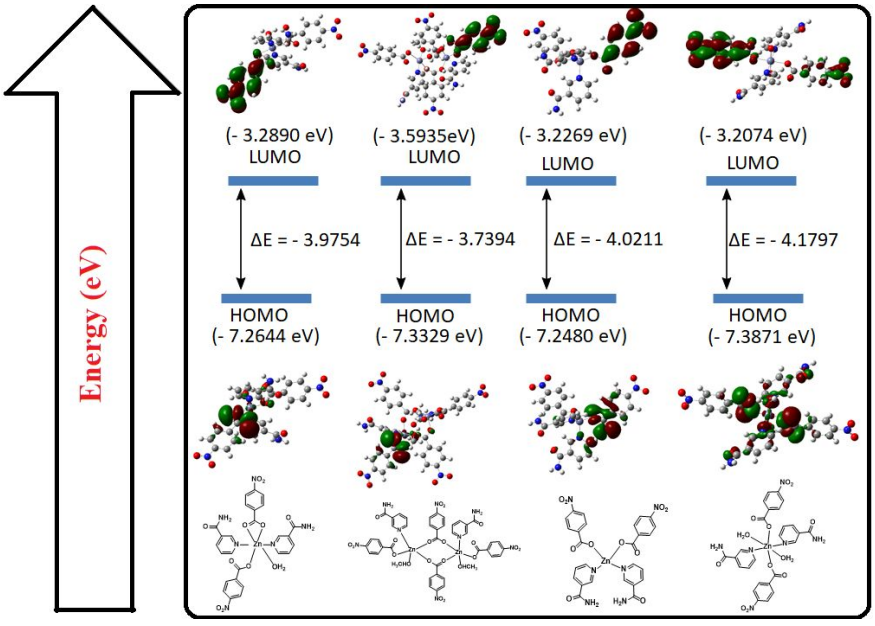

Figure S29: The HOMO and LUMO of different non-ionic zinc-complexes having pyridine-3-carboxamide 4-nitrobenzoate, calculated by DFT using B3LYP function with LANL2DZ as basis set.

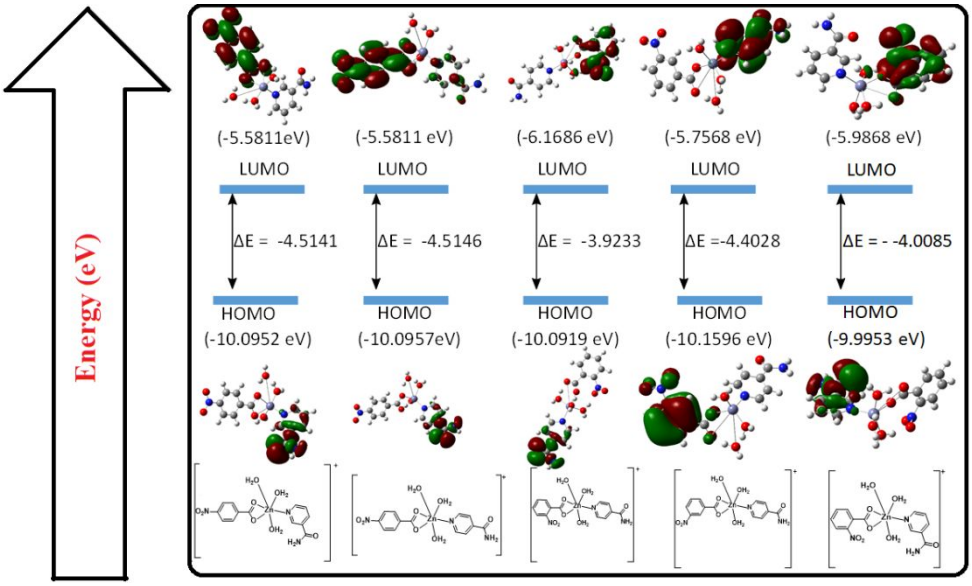

Figure S30: The HOMO and LUMO of different zinc-complexes having coordination of complex **5** (cationic form) from DFT calculation using B3LYP functional using LANL2DZ as basis set and +1 charge.

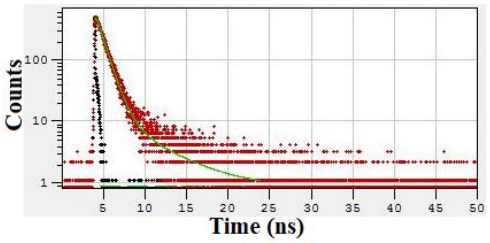

Goodness of fit χ^2: 1.006

	B_i	ΔB_i	f_i (%)	Δf_i (%)	τ_i (ns)	$\Delta\tau_i$ (ns)
1	0.0917	0.0015	88.779	2.546	0.961	0.012
2	0.0023	0.0003	11.221	1.692	4.903	0.026

Figure S31: Time resolved fluorescence emission of complex **1** (10^{-4}M) in DMSO (λ_{ex} = 375 nm, λ_{em}= 410 nm).

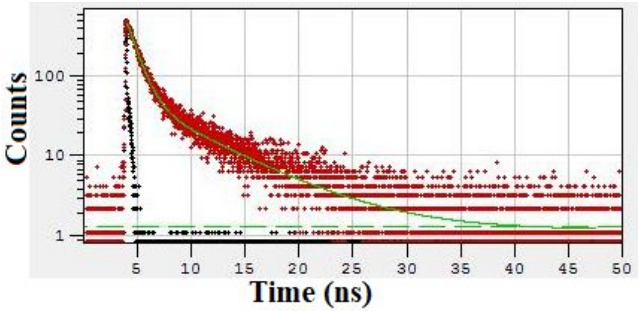

Goodness of fit χ^2: 1.002

	B_i	ΔB_i	f_i (%)	Δf_i (%)	τ_i (ns)	$\Delta\tau_i$ (ns)
1	0.0929	0.0034	64.765	3.108	0.953	0.011
2	0.0077	0.0002	35.235	0.815	6.227	0.003

Figure S32: Time resolved fluorescence emission of complex **1** (10^{-4}M) in DMSO and 50 % water (λ_{ex}= 375 nm, λ_{em}= 413 nm).

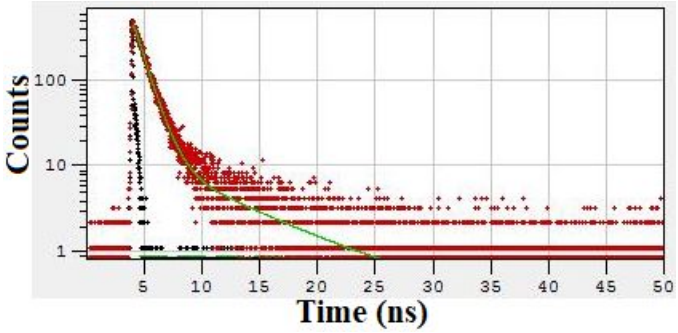

Goodness of fit χ^2: 1.058

	B_i	ΔB_i	f_i (%)	Δf_i (%)	τ_i (ns)	$\Delta\tau_i$ (ns)
1	0.0894	0.0019	86.746	2.800	0.976	0.010
2	0.0019	0.0002	13.254	1.250	6.870	0.018

Figure S33: Time resolved fluorescence emission of complex **2** (10^{-4}M) in DMSO (λ_{ex} = 375 nm, λ_{em}= 411 nm).

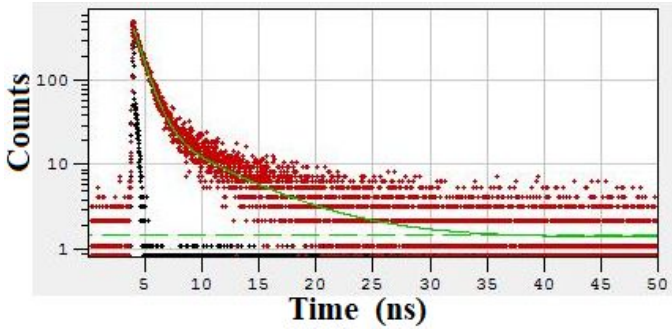

Goodness of fit χ^2: 1.029

	B_i	ΔB_i	f_i (%)	Δf_i (%)	τ_i (ns)	$\Delta\tau_i$ (ns)
1	0.0888	0.0041	76.099	4.399	0.931	0.010
2	0.0044	0.0002	23.901	0.853	5.947	0.004

Figure S34: Time resolved fluorescence emission of solution of complex **2** (10^{-4}M) in DMSO and 50 % water (λ_{ex}= 375 nm, λ_{em}= 414 nm).

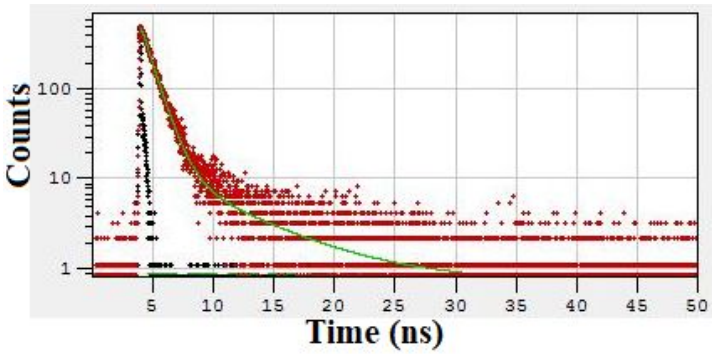

Goodness of fit χ^2: 0.993

	B_i	ΔB_i	f_i (%)	Δf_i (%)	τ_i (ns)	$\Delta\tau_i$ (ns)
1	0.0954	0.0019	87.776	2.545	0.977	0.009
2	0.0021	0.0002	12.224	1.056	6.043	0.013

Figure S35: Time resolved fluorescence emission of solution of complex 3 (10^{-4}M) in DMSO (λ_{ex}= 375 nm, λ_{em}= 411 nm).

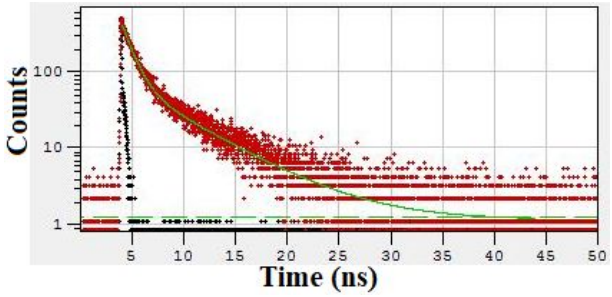

Goodness of fit χ^2: 0.995

	B_i	ΔB_i	f_i (%)	Δf_i (%)	τ_i (ns)	$\Delta\tau_i$ (ns)
1	0.0754	0.0035	55.643	3.359	0.997	0.014
2	0.0108	0.0003	44.357	1.049	5.534	0.003

Figure S36: Time resolved fluorescence emission of solution of complex **3** (10^{-4}M) in DMSO and 50 % water (λ_{ex} = 375 nm, λ_{em}= 412 nm).

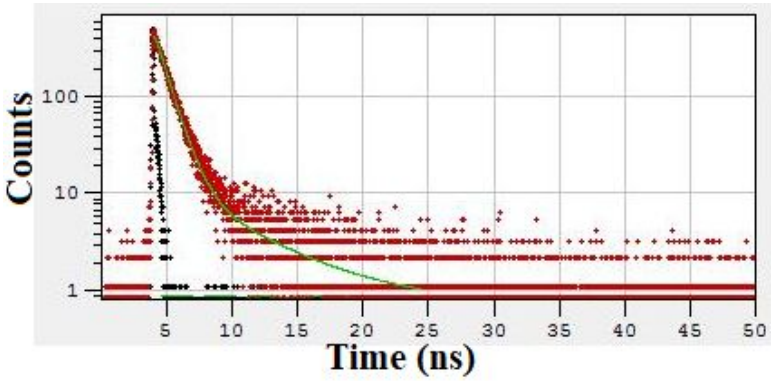

Goodness of fit χ^2: 1.018

	B_i	ΔB_i	f_i (%)	Δf_i (%)	τ_i (ns)	$\Delta\tau_i$ (ns)
1	0.0832	0.0017	87.847	2.976	0.941	0.013
2	0.0020	0.0003	12.153	1.631	5.291	0.024

Figure S37: Time resolved fluorescence emission of solution mixture of complex **4** (10^{-4}M in HPLC DMSO) (λ_{ex} = 375 nm, λ_{em} = 412 nm).

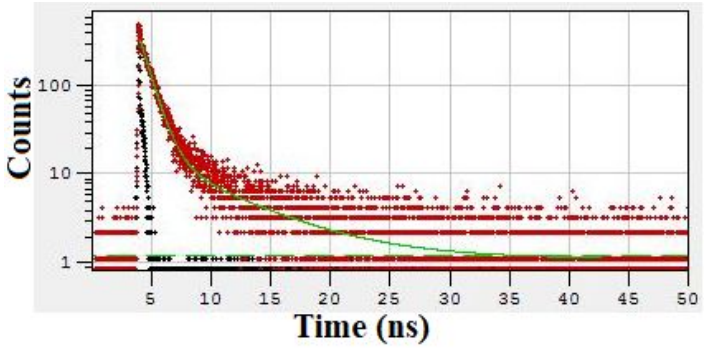

Goodness of fit χ^2: 1.008

	B_i	ΔB_i	f_i (%)	Δf_i (%)	τ_i (ns)	$\Delta\tau_i$ (ns)
1	0.0802	0.0053	82.050	6.452	0.897	0.011
2	0.0026	0.0001	17.950	0.933	6.151	0.007

Figure S38: Time-resolved fluorescence emission of solution of complex **4** (10^{-4} M) DMSO and 50% water (λ_{ex} = 375 nm, λ_{em} = 416 nm).

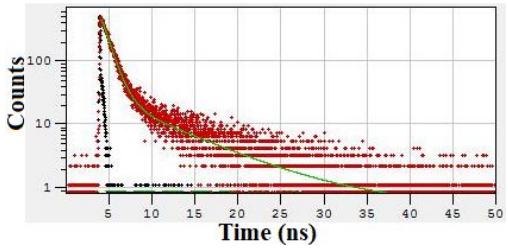

Goodness of fit χ^2: 1.088

	B_i	ΔB_i	f_i (%)	Δf_i (%)	τ_i (ns)	$\Delta\tau_i$ (ns)
1	0.0842	0.0015	74.010	2.086	0.957	0.010
2	0.0039	0.0001	25.990	0.911	7.341	0.005

Figure S39: Time-resolved fluorescence emission of solution mixture of complex **5** (10^{-4} M in DMSO) (λ_{ex} = 375 nm, λ_{em}= 412 nm).

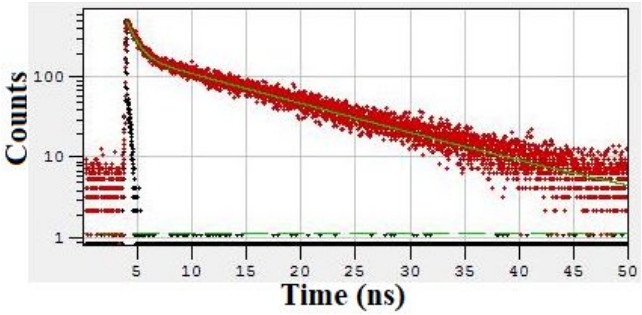

Goodness of fit χ^2: 1.118

	B_i	ΔB_i	f_i (%)	Δf_i (%)	τ_i (ns)	$\Delta\tau_i$ (ns)
1	0.0683	0.0027	16.189	1.161	0.868	0.028
2	0.0263	0.0002	83.811	0.575	11.685	0.0007

Figure S40: Time resolved fluorescence emission of solution of complex **5** (10^{-4} M) in DMSO and 50% water (λ_{ex} = 375 nm, λ_{em} = 417 nm).

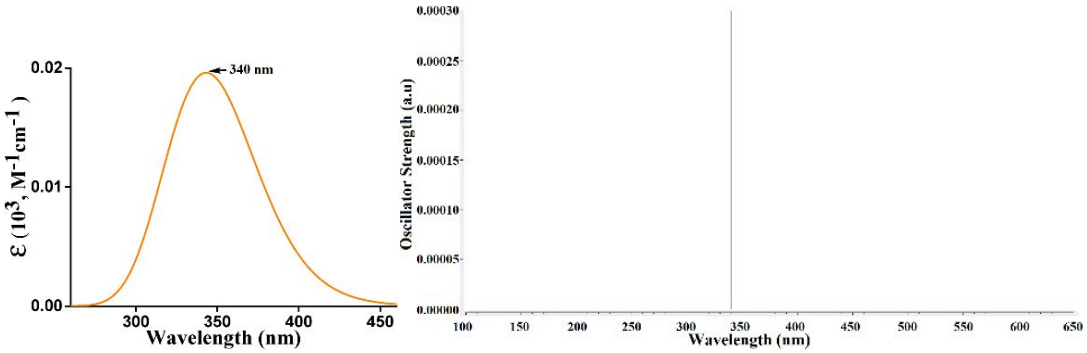

(a) (b)

Figure S41: (a) Molar absorptivity ε *vs* wavelength λ for complex **1**, (b) Oscillator strength vs wavelength λ for complex **1**, calculated by TD-DFT using B3LYP/LANL2DZ as basis set.

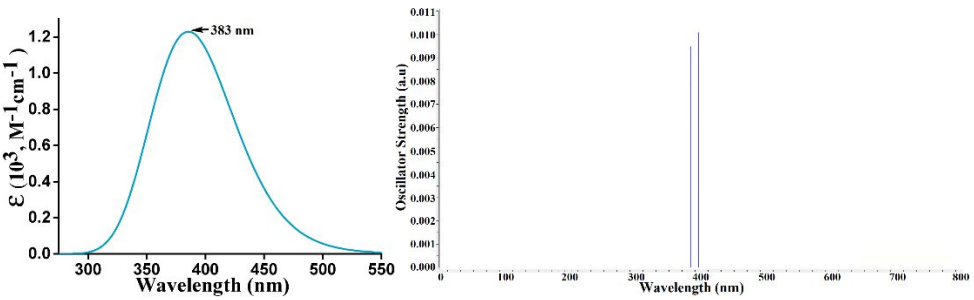

(a) (b)

Figure S42: (a) Molar absorptivity ε *vs* wavelength λ for complex **2**, (b) Oscillator strength vs wavelength λ for complex **2**, calculated by TD-DFT using B3LYP/LANL2DZ as basis set.

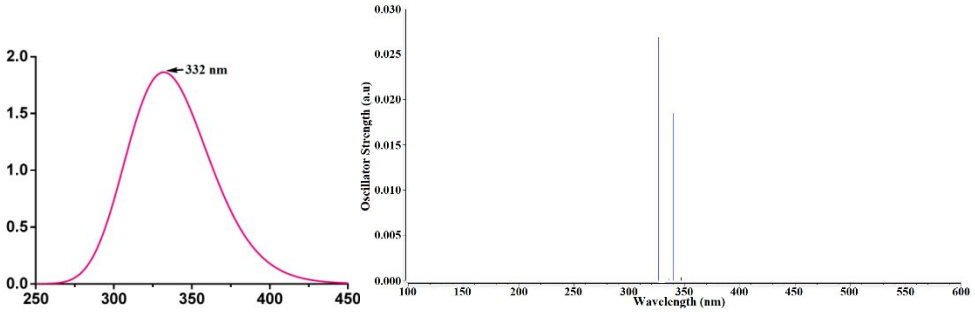

(a) (b)

Figure S43: (a) Molar absorptivity ε vs wavelength λ for complex **3**, (b) Oscillator strength vs wavelength λ for complex **3**, calculated by TD-DFT using B3LYP/LANL2DZ as basis set.

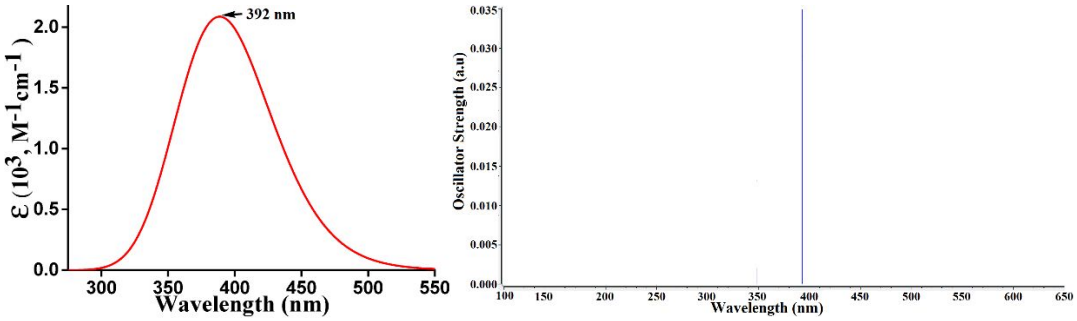

(a) (b)

Figure S44: (a) Molar absorptivity ε vs wavelength λ for complex **4**, (b) Oscillator strength vs wavelength λ for complex **4**, calculated by TD-DFT using B3LYP/LANL2DZ as basis set.

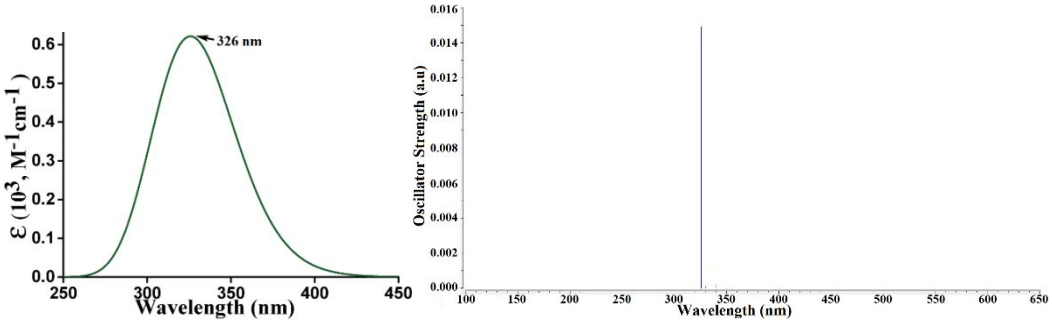

(a) (b)

Figure S45: (a) Molar absorptivity ε vs wavelength λ for complex **5**, (b) Oscillator strength vs wavelength λ for complex **5**, calculated by TD-DFT using B3LYP/LANL2DZ as basis set.

Table S3: Hydrogen bond parameters of zinc-complexes **1-5**.

Complex	D-H···A	d_{D-H} (Å)	$d_{H\cdots A}$ (Å)	$d_{D\cdots A}$ (Å)	∠D-H···A (°)
Complex 1	N(2) -H(2R) ···O(3) [1/2+x,-1/2+y,z]	0.82 (4)	2.26 (4)	3.026 (4)	155 (3)
	N(2) -H(2S) ···O(6) [x,y,z]	0.86 (4)	2.02 (4)	2.871 (4)	169 (4)
	O(6) -H(6) ···O(1) [x, 1+y, z]	0.82	1.92	2.735 (4)	170
	C(4) -H(4) …O(6) [x, y,z]	0.93	2.58	3.375 (4)	144
Complex 2	N(2)-H(2A) ···O(9) [1-x, 2-y, 1-z]	0.86	2.28	3.115(6)	164
	N(2) -H(2B) …O(7) [-x, 2-y, 1-z]	0.86	2.06	2.864 (4)	154
	N(4) -H(4R) …O(3) [-1+x,y,z]	0.80 (5)	2.43 (6)	3.106 (5)	144
	N(4) -H(4S) …O(2) [-1-x,1-y,-z]	0.92 (5)	1.95 (5)	2.853 (6)	168 (4)
	O(11)-H(11R)…O(1) [-1+x,y,z]	0.79 (6)	1.93 (6)	2.715 (5)	173 (6)
	O(11)-H(11S)…O(4) [-x,1-y,1-z]	0.83 (6)	1.89 (6)	2.707 (5)	170 (5)
	C(4)-H(4)…O(11) [1+x,y,z]	0.93	2.43	3.283 (6)	152
	C(5)-H(5)…O(3) [x,y,z]	0.93	2.47	3.038 (5)	119
	C(11)-H(11A)…O(3) [x,y,z]	0.93	2.48	3.074 (5)	122
	C(11)-H(11A)…O(5) [x,y,z]	0.93	2.48	3.255 (5)	140
Complex 3	N(4) -H(4A) ···O(5) [1-x,1-y,1-z]	0.86 (3)	2.17 (3)	3.001 (3)	162 (3)
	N(4) -H(4B) ···O(8) [1/2+x,1/2+y,z]	0.85 (3)	2.42 (4)	3.131 (4)	142 (3)
	O(9) -H(9R) ···O(5) [1-x, -y, 1-z]	0.83 (3)	1.88 (4)	2.678 (3)	161 (4)
	C(15) -H(15) …O(2) [1-x, y,1/2-z]	0.93	2.59	3.126 (3)	117
Complex 4	N(3)-H(3A) ···O(6) [-1-x,-y,-z]	0.86	2.03	2.863(2)	162
	N(3) -H(3B)…O(2) [x,y,1+z]	0.86	2.18	2.989 (2)	156
	O(5)-H(5R) …O(7) [-1+x,y,z]	0.83 (2)	1.97 (2)	2.804 (2)	177.1(19)
	O(5)-H(5S)…O(2) [x,y,z]	0.82	1.93	2.651(2)	145
	O(7)-H(7R)…O(6) [1+x,y,z]	0.84 (2)	2.07 (2)	2.887 (2)	163 (2)
	O(7)-H(7S)…O(1) [x,y,z]	0.84 (2)	2.09 (2)	2.927 (2)	178 (3)
	C(4)-H(4)…O(7) [-1/2+x,1/2-y,-1/2+z]	0.93	2.54	3.380 (3)	151
	C(9)-H(9)…O(3) [1/2+x,1/2-y,1/2+z]	0.93	2.55	3.226 (3)	130
	C(12)-H(12)…O(6) [x,y,z]	0.93	2.39	2.735 (2)	102
	C(12)-H(12)…O(1) [-x,-y,-z]	0.93	2.46	3.040 (2)	121
Complex 5	O(1)-H(1R)…O(10) [x,y,z]	0.82	1.84	2.618 (5)	158
	O(1)-H(1S)…O(9) [1+x,y,z]	0.73 (7)	2.07 (7)	2.780 (5)	166 (6)
	O(2)-H(2R) ···O(1) [x,y,z]	0.82	2.58	2.853(5)	101
	O(2) -H(2R)…O(9) [x,y,z]	0.82	1.89	2.643 (4)	152
	O(2)-H(2S)…O(5) [-1+x,y,z]	0.85 (4)	1.98 (4)	2.789 (4)	160 (4)
	N(3)-H(3F)…O(4) [1+x,-1+y,z]	0.84 (6)	2.10 (6)	2.925(6)	167 (6)
	N(3)-H(3G)…O(9) [1+x,y,z]	0.89 (5)	2.29 (5)	3.165 (5)	168 (5)
	O(3)-H(3R)…O(8) [-1+x,y,z]	0.82	1.97	2.789 (5)	178
	O(3)-H(3S)…O(6) [2-x,1-y,-z]	0.85 (3)	2.15 (4)	2.949 (6)	158 (5)
	C(4)-H(4)…O(7) [2-x,2-y,-z]	0.93	2.48	3.319 (10)	151
	C(8)-H(8)…O(12) [-x,1-y,1-z]	0.93	2.59	3.473 (7)	158
	C(10)-H(10)…O(9) [1+x, -1+y,z]	0.93	2.53	3.426 (6)	163
	C(12)-H(12)…O(5) [x,y,z]	0.93	2.55	3.139 (6)	122
	C(12)-H(12)…O(8) [x,y,z]	0.93	2.47	2.799 (6)	101
	C(16)-H(16)…O(9) [x,y,z]]	0.93	2.50	2.814 (6)	100